

# Journal of Engineering Research

## DEVELOPMENT, MODELING AND EXPERIMENTAL VALIDATION OF A SIX- DEGREES-OF-FREEDOM ROBOT ARM

---

*Juan Reyes-Luévano*

TecNM/Instituto Tecnológico de  
Aguascalientes  
México

*J. A. Guerrero-Viramontes*

TecNM/Instituto Tecnológico de  
Aguascalientes  
México

*M. Funes-Gallanzi*

Ardita México S. A. de C. V.  
Mexico

All content in this magazine is licensed under a Creative Commons Attribution License. Attribution-Non-Commercial-Non-Derivatives 4.0 International (CC BY-NC-ND 4.0).



**Abstract:** This paper presents the development, modeling and experimental validation of a six-degrees-of-freedom robot arm with revolute-type links and a spherical wrist. The robot's design allows for a load handling capacity of 400 grams, it has high repeatability (+/- 1 mm), and its dynamics can be configured by software to generate trajectories with a desired velocity and acceleration profile. The estimation of the position and orientation of the end effector given the angular position of the links is based on the Denavit-Hartenberg method. In this sense, an inverse kinematics model based on the geometric method is proposed to efficiently estimate the necessary parameters for the robot to execute a specific trajectory. Simulation results and experimental tests validate the proposed kinematics models and the robot trajectory execution scheme. As a result, the six-degree-of-freedom robot can be safely implemented in exploration tasks, recognition (using artificial vision systems) and manipulation of small parts (pieces and objects).

**Keywords:** Robot arm, direct kinematics, inverse kinematics, modeling, geometric method, Denavit-Hartenberg method.

## INTRODUCTION

The growing complexity of exploration tasks (diagnosis and inspection), as well as the high demand for automated systems for applications based on artificial intelligence [1]; make it necessary to develop and improve manipulative systems (robots). In this sense, it is desirable that a manipulator has a low implementation cost, high performance and high reliability.

There are mainly two fields that represent an important area of opportunity for robots with the aforementioned characteristics. In the industrial field, the implementation of non-destructive inspection methods in quality control tasks, as well as flexible manufacturing

processes; those require robots with high manipulative capacity and highly adaptable to various tasks that fluctuate in complexity [2-5]. On the other hand, in the area of medical services, the implementation of telemedicine systems for exploration, control, monitoring and diagnosis of patients; has shown the need for high-reliability and low-cost compact manipulators, which can be used as the basis of a remote personalized health service system [6].

Based on the above, this work addresses the process of development, modeling and experimental validation of an anthropomorphic manipulator with six degrees of freedom. The results indicate that the robot prototype has a low implementation cost, high repeatability (1mm), smooth dynamics, and the ability to handle 400 grams of load. The performance and characteristics of the prototype make it ideal to be safely implemented in exploration tasks (medical or non-destructive optical tests), recognition by artificial vision and small works involving the manipulation of parts or objects.

## BACKGROUND

The six - degree - of - freedom anthropomorphic manipulator has a body, elbow, arm, wrist, and end-effector structure. See Fig.1.1. These characteristics make it have a high handling capacity. The series topology with links of the revolute type and spherical wrist, is widely used due to the possibility of decoupling the estimation of the final effector coordinate in two parameters, position and orientation.

The direct kinematics of the robot allows to determine the position and orientation of the final link of the manipulator from the angle of each of the axes:  $q_i$ . For this, the Denavit-Hartenberg algorithm [7] is used. The transformation matrix for any chain of links ( $T_{(i-1)/i}$ ) of the frame of reference ( $x_0, y_0,$

$z_0$ ) to the  $i$ -th axis, is given by (1). For a series of translations (*Trans*) y rotations (*Rot*) on the axis  $z$  and  $x$ . Hence, the forward kinematics for the entire robot link chain is given by (2). See Fig. 1.1. Where the position of the end effector of the robot is given by the vector  $\vec{p}=(p_x, p_y, p_z)$  and the orientation by the matrix  $(\vec{n}, \vec{o}, \vec{a})$ . In (1), C denotes cosine and S to the sine function. This way, the parameters:  $\alpha_i$  and  $\theta_i$  set the position:  $\vec{p}=(x,y,z)$  from the end of the robot. See Figure 1.2.

$$T_{(i-1)/i} = Rot_z(\theta_i)Trans_{x,y,z}(a_i, 0, d_i)Rot_x(\alpha_i) \quad (1)$$

$$T_{(i-1)/i} = \begin{bmatrix} C\theta_i & -S\theta_i C\alpha_i & S\theta_i S\alpha_i & a_i C\theta_i \\ S\theta_i & C\theta_i C\alpha_i & -C\theta_i S\alpha_i & a_i S\theta_i \\ 0 & S\alpha_i & C\alpha_i & d_i \\ 0 & 0 & 0 & 1 \end{bmatrix}$$

$$H = T_{(0)/6} = \begin{bmatrix} R_{11} & R_{12} & R_{13} & x \\ R_{21} & R_{22} & R_{23} & y \\ R_{31} & R_{32} & R_{33} & z \\ 0 & 0 & 0 & 1 \end{bmatrix} = \begin{bmatrix} n_x & o_x & a_x & p_x \\ n_y & o_y & a_y & p_y \\ n_z & o_z & a_z & p_z \\ 0 & 0 & 0 & 1 \end{bmatrix} = \begin{bmatrix} R & O \\ 0 & 1 \end{bmatrix} \quad (2)$$

The inverse kinematics of the robot allows estimating the necessary value of the angular position of the links  $q_i$  so that the final effector is positioned at the coordinate  $(p_x, p_y, p_z)$ . The decoupling process of the inverse kinematics problem involves knowing a priori the orientation of the end effector. That is, knowing the angular value of the links of the robot wrist ( $q_4, q_5, q_6$ ) that define the orientation of the end effector. Based on this, the estimation of the links ( $q_1, q_2, q_3$ ) leads to a set of equations given by expression (5). The solution of these nonlinear equations is carried out numerically, so the computational cost involved is high, coupled with the existence of multiple solutions. In this sense, a closed solution for inverse kinematics based on the geometric method is more effective.

$$T_{0/6} = T_{0/1} \cdot T_{1/2} \cdot T_{2/3} \cdot T_{3/4} \cdot T_{4/5} \cdot T_{5/6} = T_{0/3} \cdot T_{3/6} \quad (3)$$

$$T_{3/6} = T_{3/4} \cdot T_{4/5} \cdot T_{5/6} = \begin{bmatrix} R_{3/6} & O_{3/6} \\ 0 & 1 \end{bmatrix} \quad (4)$$

$$T_{0/3} = T_{0/6} \cdot [T_{3/6}]^{-1} \quad (5)$$

## EXPERIMENTAL DESIGN

This work focuses its attention on the development, modeling and experimental validation of an anthropomorphic manipulator with six degrees of freedom. This is mainly due to its high capacity for handling the final effector in a reduced work area. Figure 1.1 presents the schematic of the robot used in the experimental tests. The overall design consists of a series topology, with revolute type joints and spherical wrist. Given the mechanical specifications of the actuators, their load handling capacity is approximately 400 grams.

Estimation of the position and orientation of the end effector:  $P(p_x, p_y, p_z)$  it is approached from the direct kinematics of the robot. For its part, knowledge of the angular position of the links:  $q_i$  so that the end effector is positioned at an arbitrary point  $P(p_x, p_y, p_z)$ ; it is substantiated on a proposal based on the geometric method to provide a solution to the inverse kinematics of the robot. In the case of direct kinematics, the formalism used to estimate the angular position of the links corresponds to the Denavit-Hartenberg algorithm. This formulation entails obtaining a homogeneous transformation matrix based on the analysis of the reference frames and axes of the robot. As a result, a submatrix of rotation  $R$  and a position vector  $O$  of the end effector are obtained, given a priori knowledge of the angular position of the robot links. On the other hand, the solution of the inverse kinematics of the robot based on the homogeneous transformation matrix leads to a system of nonlinear equations whose solution is normally not feasible to be implemented in real time, mainly due to

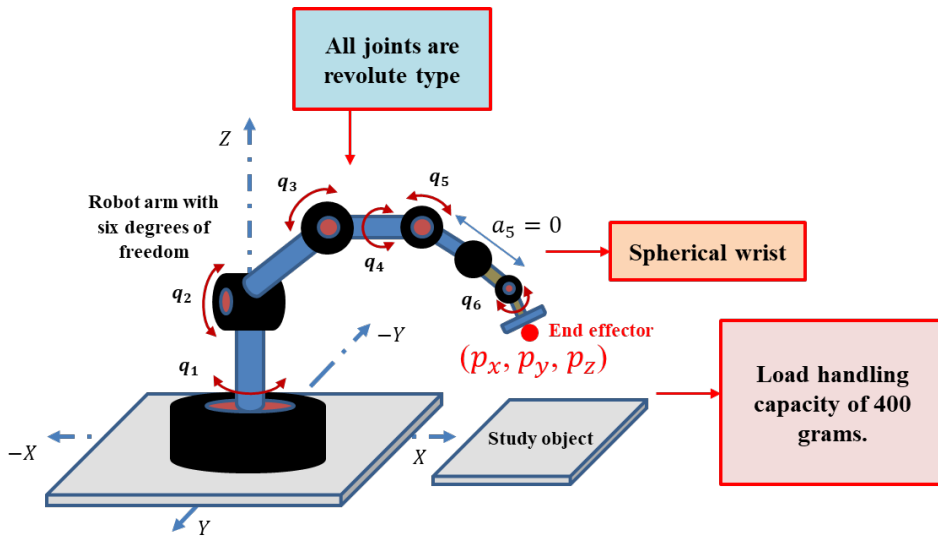


Figure 1.1 Anthropomorphic robot with six degrees of freedom in serial topology.

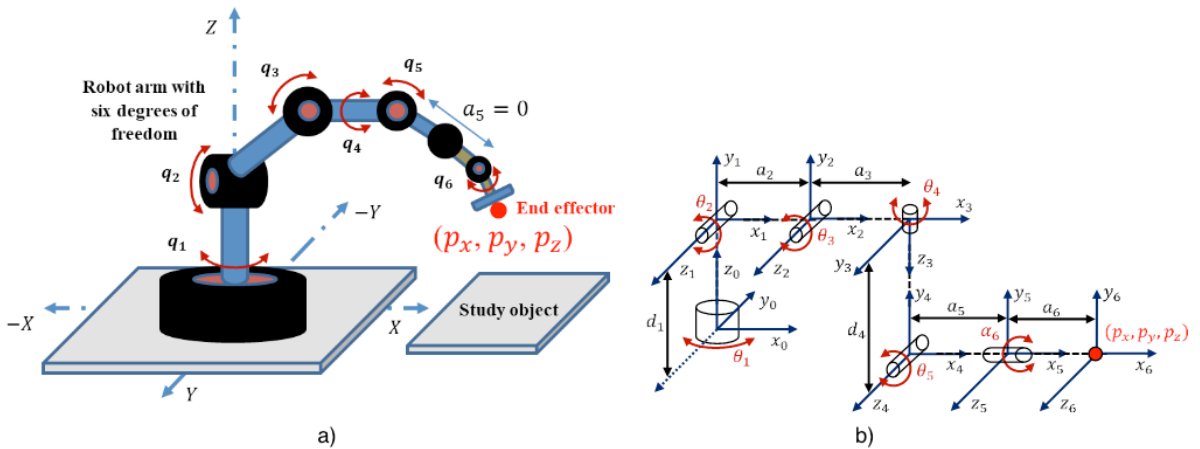


Figure 1.2 a) Topology, and b) reference frames and robot axes.

Link	$\theta_i$	$d_i$	$a_i$	$\alpha_i$	$\theta_1$	$\theta_2$	$\theta_3$	$\theta_4$	$\theta_5$	$\alpha_6$	$p_x$	$p_y$	$p_z$
1	$\theta_1$	$d_1$	0	$90^\circ$	21	70	-50	0	0	0	184.8892	70.9723	190.56
2	$\theta_2$	0	$a_2$	0	15	50	-20	10	10	10	280.7466	71.0299	182.1015
3	$\theta_3$	0	$a_3$	$90^\circ$	0	30	-10	20	20	20	302.7067	-7.6170	104.8934
4	$\theta_4$	$d_4$	0	$-90^\circ$	30	20	0	30	30	30	277.0058	148.0794	74.1577
5	$\theta_5$	0	$a_5$	0	60	20	0	30	30	30	165.8544	266.7434	74.1577
6	0	0	$a_6$	$\alpha_6$	60	0	20	50	30	60	174.7628	271.2523	0.7663

Table 1. Denavit-Hartenberg parameters for the six-degree-of-freedom revolute-type manipulator with spherical wrist, and end-effector position estimation results.

the complexity, computational cost and the existence of multiple solutions. In this context, the inverse kinematics solution based on the geometric method is a more feasible option.

## RESULTS

The direct kinematics analysis of the manipulator presented in Fig. 1.2 a) is based on the diagram of the reference systems and axes of the robot, shown in Fig. 1.2 b). The estimation of the position and orientation of the final effect can be approached using expression (6). Table 1 presents the homogeneous transformation parameters and the results of the coordinate estimation  $P(p_x, p_y, p_z)$  of the final effector, for a set of angular values  $q_i$  for robot links.

The inverse kinematics solution proposed in this work is closed and is based on the geometric method. For each topology of the robot (defined by the region of operation of each link of the shoulder and the elbow) the expressions that allow calculating the value of the angular position for the first three links of the robot are proposed. See Figure 1.3.

$$T_{(i-1)/i} = \begin{bmatrix} C\theta_i & -S\theta_i C\alpha_i & S\theta_i S\alpha_i & a_i C\theta_i \\ S\theta_i & C\theta_i C\alpha_i & -C\theta_i S\alpha_i & a_i S\theta_i \\ 0 & S\alpha_i & C\alpha_i & d_i \\ 0 & 0 & 0 & 1 \end{bmatrix} = \begin{bmatrix} n_x & o_x & a_x & p_x \\ n_y & o_y & a_y & p_y \\ n_z & o_z & a_z & p_z \\ 0 & 0 & 0 & 1 \end{bmatrix} = \begin{bmatrix} R & 0 \\ 0 & 1 \end{bmatrix} \quad (6)$$

For each region of operation of the robot's shoulder and elbow links, the necessary expressions for the estimation of the first three links of the manipulator are proposed. The equations are derived under consideration of decoupling of the spherical wrist and a priori knowledge of the orientation of the end effector given by the links:  $q_4, q_5, q_6$ . Due to the effective arm of the fourth link:  $d_4$  and given that the position:  $P_{e4}$  is independent of the angular value of the fourth link, the position of the end effector can be considered to be the

coordinate point: . Therefore, executing an end effector trajectory entail estimating the angular values of the first three links ( $q_1, q_2, q_3$ ) based on a series of points  $P_{e4}$  contained within the trajectory. See Fig. 1.3. Table 1.2 presents the results of the estimation of the angular position of the links from the inverse kinematics solution, given a specific path of the robot.

For an elbow down arrangement (see Fig. 1.3 a), the expressions that allow estimating the angular position of the first three links of the robot based on the coordinate point  $P_{e4i}$  are:

$$\begin{aligned} \theta_1 &= \cos^{-1} \left( \frac{x_{c3}}{r} \right) \\ \theta_2 &= \sin^{-1} \left( \frac{mB^2 + a_2^2 - a_3^2}{2mBa_2} \right) \\ \theta_3 &= \cos^{-1} \left( \frac{e^2 + a_3^2 - d^2}{2ea_3} \right) \end{aligned} \quad (7)$$

$$\begin{aligned} P_{d4v} &= d_4 \sin(y) \\ P_{d4h} &= d_4 \cos(y) \\ n_r &= r + P_{d4h} \\ p_{z4} &= P_{Az} = S - P_{d4v} \\ p_{x4} &= n_r \cos(\theta_1) \\ p_{y4} &= n_r \sin(\theta_1) \end{aligned}$$

For an elbow-up arrangement and  $\theta_3=0$  (see Fig. 1.3 b)), the estimation of the angular position of the first and second link is given by (8), considering the position of the end effector:  $P_{e4i}$ .

$$\begin{aligned} \theta_1 &= \cos^{-1} \left( \frac{x_{c4}}{n_r} \right) \\ \theta_2 &= \sin^{-1} \left( \frac{z_{c3} - d_1}{a_2 + a_3} \right) \\ \theta_3 &= 0 \end{aligned} \quad (8)$$

For an elbow-up arrangement and  $\theta_2 > 90^\circ$  (see Fig. 1.3 c)), the angular position of the first three links can be described by (9).

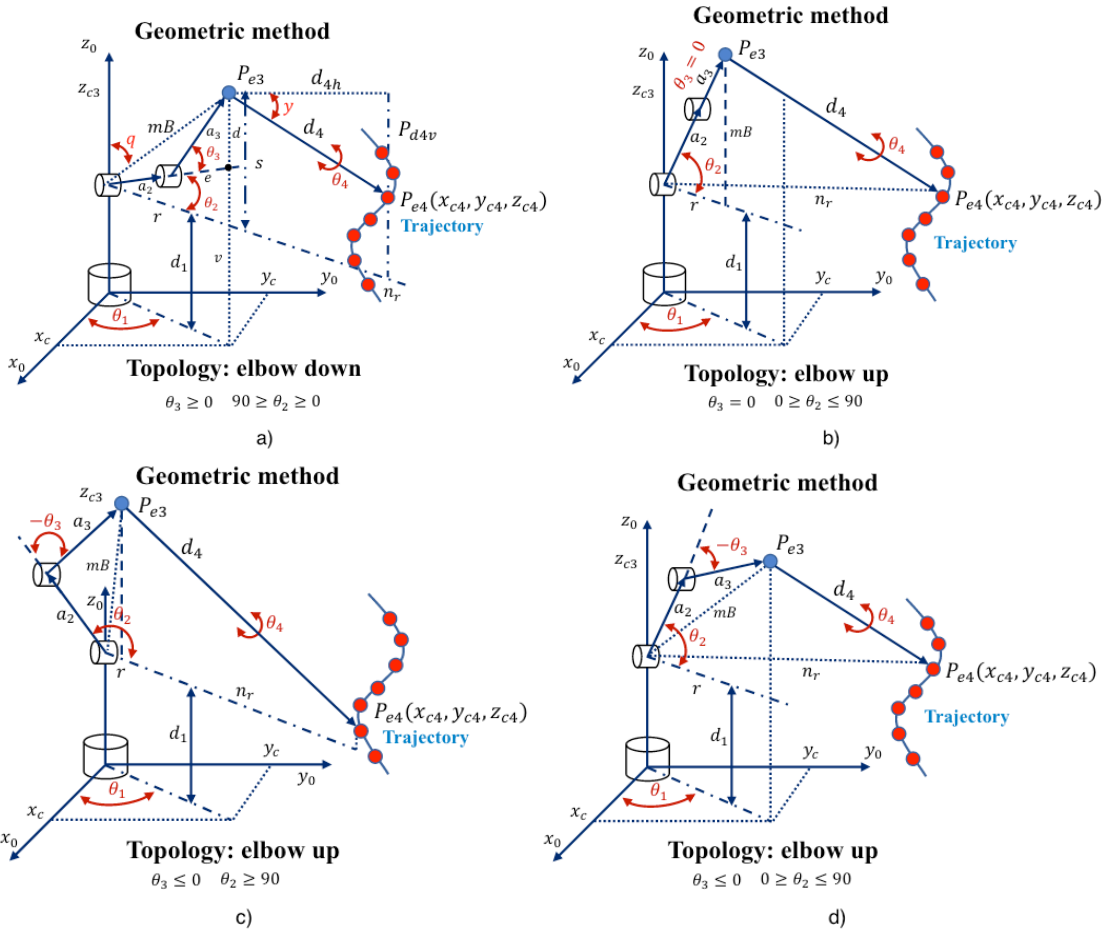


Figure 1.3 Topologies of the robot in relation to the region of operation of each link of the shoulder and elbow.

Trajectory			Link estimation					
$p_x$	$p_y$	$p_z$	$\theta_1$	$\theta_2$	$\theta_3$	$\theta_4$	$\theta_5$	$\alpha_6$
-94.8271	0	403.4645	180	66.5639	1.2996	0	-90	0
-79.0226	52.4176	403.4645	146.4427	66.5639	1.2996	0	-90	0
-63.2180	70.6799	403.4645	131.8103	66.5639	1.2996	0	-90	0
-47.4135	82.1227	403.4645	120	66.5639	1.2996	0	-90	0
-31.6090	89.4038	403.4645	109.4712	66.5639	1.2996	0	-90	0
-15.8045	93.5008	403.4645	99.5941	66.5639	1.2996	0	-90	0
0	94.8271	403.4645	90	66.5639	1.2996	0	-90	0

Table 2. Estimation of the angular position of the links ( $q_1, q_2, q_3$ ) of the robot for trajectory execution. The solution of the inverse kinematics is approached from the geometric method approach.

$$\begin{aligned}\theta_1 &= \cos^{-1}\left(\frac{x_{c4}}{n_r}\right) \\ \theta_2 &= \cos^{-1}\left(\frac{mB^2 + a_2^2 - a_3^2}{2mBa_2}\right) + \sin^{-1}\left(\frac{|r|}{mB}\right) + \left(\frac{\pi}{2}\right) \\ \theta_3 &= \cos^{-1}\left(\frac{a_3^2 + a_2^2 - mB^2}{2a_3a_2}\right) - (\pi)\end{aligned}\quad (9)$$

Finally, for an elbow-up arrangement and  $\theta_2 \leq 90^\circ$  (see Fig. 1.3 d)), the angular position of the links ( $q_1, q_2, q_3$ ) is given by (10).

$$\begin{aligned}\theta_1 &= \cos^{-1}\left(\frac{x_{c4}}{n_r}\right) \\ \theta_2 &= \sin^{-1}\left(\frac{z_{p3} - d_1}{mB}\right) + \cos^{-1}\left(\frac{a_2^2 + mB^2 - a_3^2}{2a_2mB}\right) \\ \theta_3 &= \cos^{-1}\left(\frac{a_2^2 + a_3^2 - mB^2}{2a_2a_3}\right) - (\pi)\end{aligned}\quad (10)$$

The robot trajectory execution scheme based on inverse and forward kinematics, is presented in Fig. 1.4 a). This implementation makes it possible to discriminate those points of the final effector trajectory that are outside the robot's work region. Fig. 1.4 b) shows the simulation of the execution of a trajectory of the end effector of the robot.

The prototype of the robot used in the experimental tests is presented in Fig. 1.5 b). The block diagram of Fig. 1.5 a) describes in detail the different electronic, control, communication, and user interface systems of the robot with six-degrees-of-freedom. In order to validate the forward and inverse kinematics model, trajectory execution tests were conducted. Fig. 1.6 shows the execution of a sequence of robot positions that make up a path.

## CONCLUSIONS

In this work, the development, modeling and experimental validation of a six-degrees-of-freedom robot arm with revolute-type joints and a spherical wrist were presented. The estimation of the position and orientation of the final effector was approached from

the direct and inverse kinematics of the robot. In this sense, a modeling proposal for inverse kinematics is presented, and it is characterized by being a simple formulation, fast in execution and easy to implement in software.

The experimental tests showed that the proposed scheme for the execution of trajectories is functional. The results indicate that the robot prototype has a low implementation cost, high repeatability (1mm), smooth dynamics, and the ability to handle 400 grams of load. The performance and characteristics of the prototype make it ideal to be safely implemented in exploration tasks (medical or non-destructive optical tests), recognition by artificial vision and small works involving the manipulation of parts or objects.



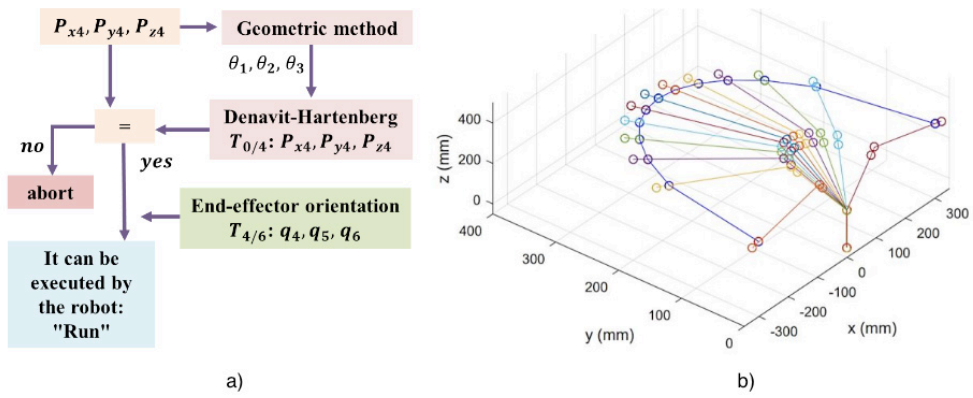


Figure 1.4 a) Robot execution scheme. b) Simulation of trajectory execution.

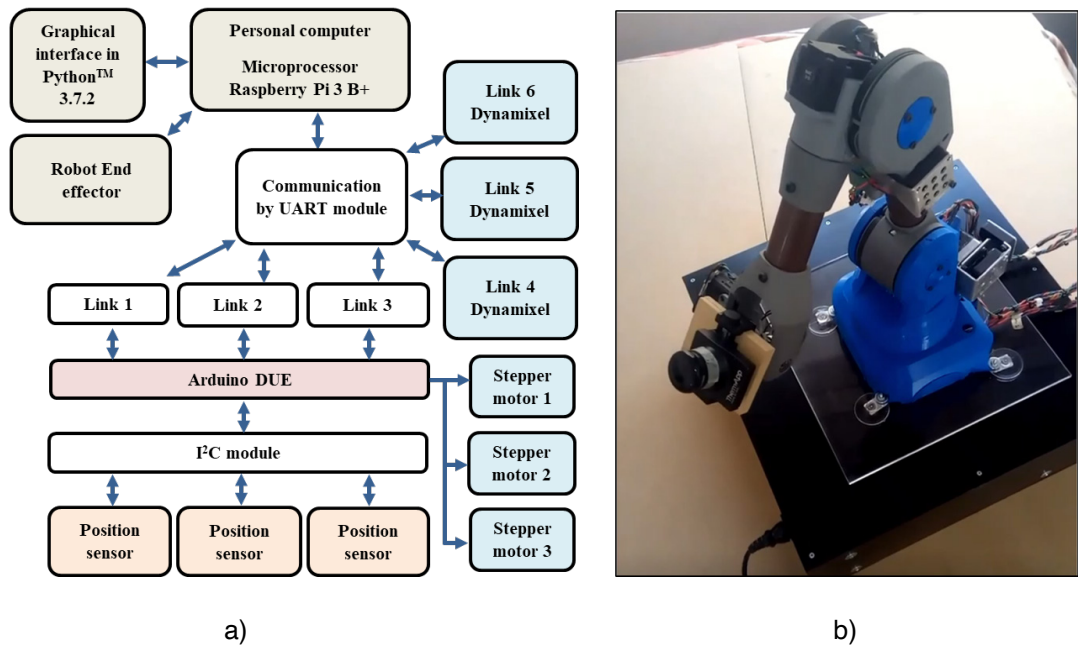


Figure 1.5 a) Block diagram of the robot systems. b) Prototype of the robot used in the experimental tests.

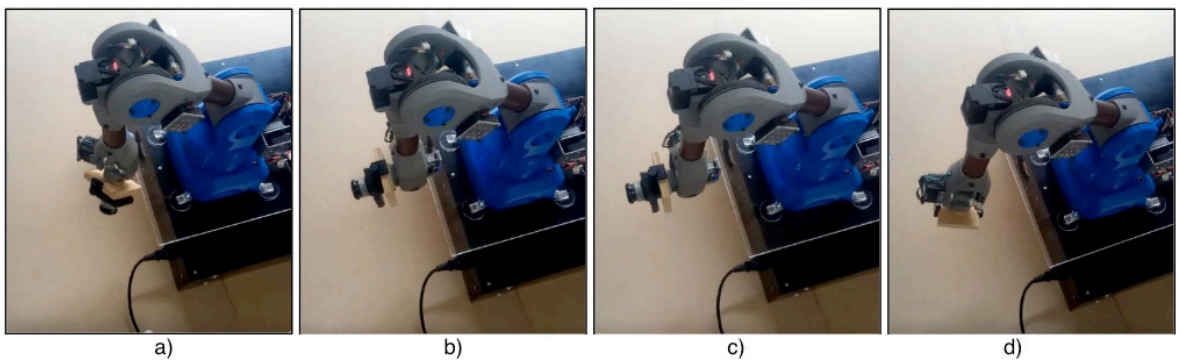


Figure 1.6 Experimental test of the execution of a trajectory in the final effector of the robot.



## REFERENCES

1. L. Zongxing, X. Chunguang, P. Qinxue, Z. Xinyu, L. Xinliang, "Inverse Kinematic Analysis and Evaluation of a Robot for Nondestructive Testing Application", *Journal of Robotics*, Vol. 1, 1, 2015, pp. 1-6.
2. Patel K. B., Zalte M. B., Panchal S. R., "A Review: Machine vision and its applications", *IOSR J. of Electron. and Comm. Eng.*, Vol. 7, 5, 2013, pp. 72-77.
3. Kumar A., "Computer Vision-based Fabric Defect Detection: A Survey", *IEEE Trans. On Ind. Electron.*, Vol. 55, 1, 2008, pp. 348-363.
4. Malik A. A., Andersen M. V., "Advances in machine vision for flexible feeding of assembly parts", *Procedia Manufacturing*, Vol. 38, 1, 2019, pp. 1228-1235.
5. Chauhan V., Surgenor B., "A Comparative Study of Machine Vision Based Methods for Fault Detection in an Automated Assembly Machine", *Procedia Manufacturing*, Vol. 1, 1, 2015, pp. 416-428.
6. S. Bagavathiappan, B. B. Lahiri, T. Saravanan, J. Philip y T. Jayakumar, "Infrared thermography for condition monitoring- A review", *Infrared Physics and Technology*, Vol. 60, 1, 2013, pp. 35-55.
7. J. Denavit, R. S. Hartenberg. "A Kinematic Notation for Lower-Pair Mechanism Based on Matrices", *Journal of Applied Mechanics*, Vol. 22, 1, 1955, pp. 215-221.